

Model of planar refractometer based on a two-port interferometer in glass

M. BŁAHUT, M. ROGOZIŃSKI, K. GUT, P. KARASIŃSKI, A. OPILSKI

Institute of Physics, Silesian Technical University, ul. Bolesława Krzywoustego 2, 44–100 Gliwice, Poland.

In the paper, the technology and testing of the planar refractometer made by the $K^+ - Na^+$ ion-exchange in glass, based on a symmetrical configuration of a two-port Mach–Zehnder (MZ) interferometer, are presented. The influence of the technological process parameters and interferometer geometry on optical characteristics of the planar refractometer is examined.

1. Introduction

The planar Mach–Zehnder interferometers in glass have found important applications in integrated optical circuits [1], as the elements of wavelength demultiplexers and filters, ring resonators, all-optical switches and single-mode optical sensors. Optical properties of such structures depend on their fabrication parameters. A knowledge relating the optical response of the interferometers to the technological parameters is essential in designing devices with required characteristics.

In the paper, studies on the application of the symmetrical MZ interferometer configuration in the planar refractometer technology are presented. The refractometer was made by the $K^+ - Na^+$ ion-exchange in borosilicate glass. Our investigations concerned the single-mode channel waveguides technology, the optimization of the planar interferometer geometry and the determination of optical characteristics of the refractometer.

2. $K^+ - Na^+$ ion-exchange

The $K^+ - Na^+$ ion-exchange technique in glass is a widely used method of producing passive integrated optical components [2], [3]. Waveguide structures are characterized by low material loss and high thermal stability, and a small refractive index change distinguishes this process in single-mode application.

The basis of every $K^+ - Na^+$ ion-exchange process is the phenomenon of two-component diffusion, described by the following equation [4]:

$$\frac{\partial C_K}{\partial t} = \nabla \left[\frac{D_K}{1 - (1 - m)C_K} \nabla C_K \right] - \mu_K f E_0 \nabla \left[\frac{C_K}{1 - (1 - m)C_K} \right] \quad (1)$$

where C_K is the normalized K^+ ion concentration ($C_K + C_{Na} = 1$), m is the mobility ratio of the ions K^+ and Na^+ , D_K and μ_K denote self-diffusion coefficient and

mobility of ions K^+ , respectively, E_0 is the external electric field ($E_0 = 0$ for pure thermal diffusion), f is the coefficient of correlation for the ion mobility.

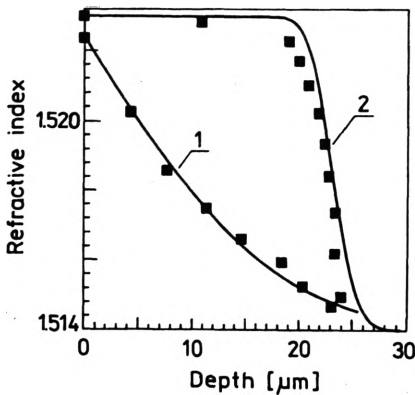
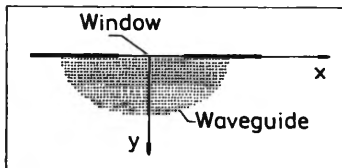


Fig. 1. Refractive index distributions of planar waveguides obtained during diffusion (1 - $t_D = 60$ h, $T = 400$ °C), and electrodiffusion (2 - $t_D = 1$ h, $T = 400$ °C, $E_0 = 30$ V/mm) of K^+ ions measured by the IWKB method

Material parameters of Equation (1): D_K , m , f and the maximum of the refractive index change Δn can be determined by measurements of respective planar index profiles using IWKB method. Figure 1 presents typical refractive index distributions of waveguides obtained during diffusion and electrodiffusion of K^+ ions from molten pure KNO_3 to borosilicate glass ($n = 1.5142$). The best matching was obtained for the following parameters of the process: $D_K = 1.61$ $\mu m^2/h$, $f = 15$, $\Delta n = 0.0084$, $m = 1$.



▲

Fig. 2. Geometry of the ion-exchange process

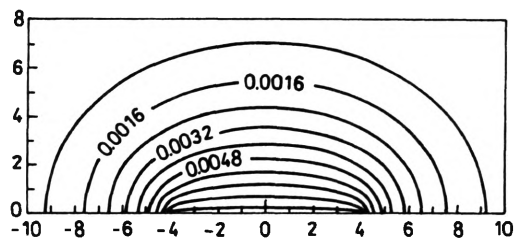


Fig. 3. Theoretical distribution of the refractive index profile obtained in the diffusion process ($t_D = 1$ h, $T = 400$ °C) through the window of 9 μm in width (vertical and horizontal dimensions in μm)

In order to optimize technological parameters required in production of single-mode channel waveguides, the numerical simulation of the thermal diffusion process for the different mask widths was performed for the geometry shown in Fig. 2. In Figure 3, a typical refractive index profile obtained as a result of thermal

diffusion continued for 8 hours through the window of 9 μm in width is presented. The asymmetry of the index distribution observed may exert influence on polarization properties of the waveguide.

Modal properties of such waveguide structures were determined by an effective index method [4] and the domains of single-mode light propagation were determined as a function of the technological process parameters (mas width, time and temperature). Figure 4 presents the dependence of numerically calculated effective indices of basic waveguide modes (at $\lambda = 1.3 \mu\text{m}$) of channel waveguides produced by pure diffusion process through the opening of 9 μm in width on the profile depth $\sqrt{D_K t_D}$. The single-mode regime extends over the time of 3 h–11 h.

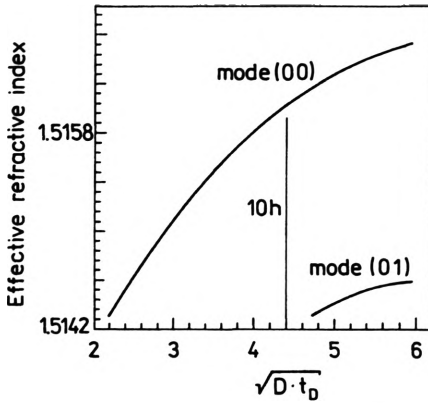


Fig. 4. Dependence of numerically calculated effective indices (for explanation see text)

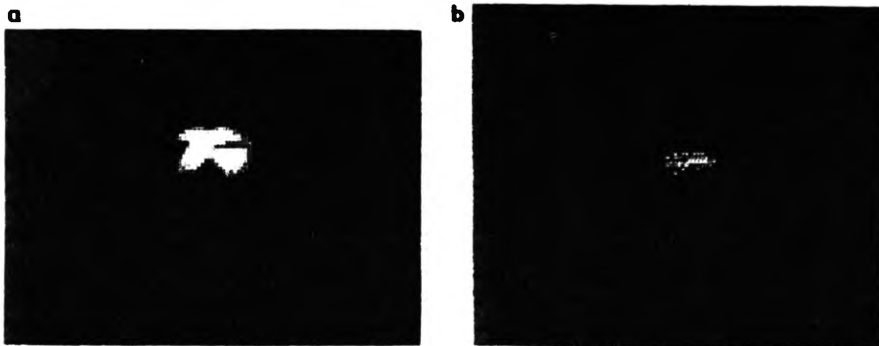


Fig. 5. Near-field pattern in the output of the channel waveguide excited by the light of the wavelength: a – $\lambda = 0.6328 \mu\text{m}$, b – $\lambda = 1.3 \mu\text{m}$

On the grounds of the above, the single-mode channel waveguides can be fabricated. Figure 5a,b shows the near-field pattern at the output of the channel waveguide produced by the $\text{K}^+ - \text{Na}^+$ ion exchange continued for 10 hours ($T = 400^\circ\text{C}$) through the opening in an aluminium mask of 8 μm in width, excited by the light of the wavelength $\lambda = 0.6328 \mu\text{m}$ and 1.3 μm , respectively. The results obtained

indicate that the waveguide structure guides a few modes at $\lambda = 0.6328 \mu\text{m}$ (the field distribution of the output depends on the field distribution of the input) and is a single-mode one at $\lambda = 1.3 \mu\text{m}$.

3. Planar refractometer technology

The planar refractometer was made in the symmetrical MZ interferometer configuration. The interferometers were produced by the ion-exchange process described above. Figure 6 depicts schematically the mask configuration. The width of the openings is $9 \mu\text{m}$ and the length of the whole waveguide structure is about 4.5 cm . An ion-exchange time, $t_D = 8 \text{ h}$, was chosen in order to obtain a single-mode operation at $\lambda = 1.3 \mu\text{m}$.

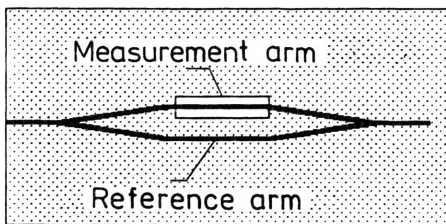


Fig. 6. Topology of the symmetrical MZ interferometer

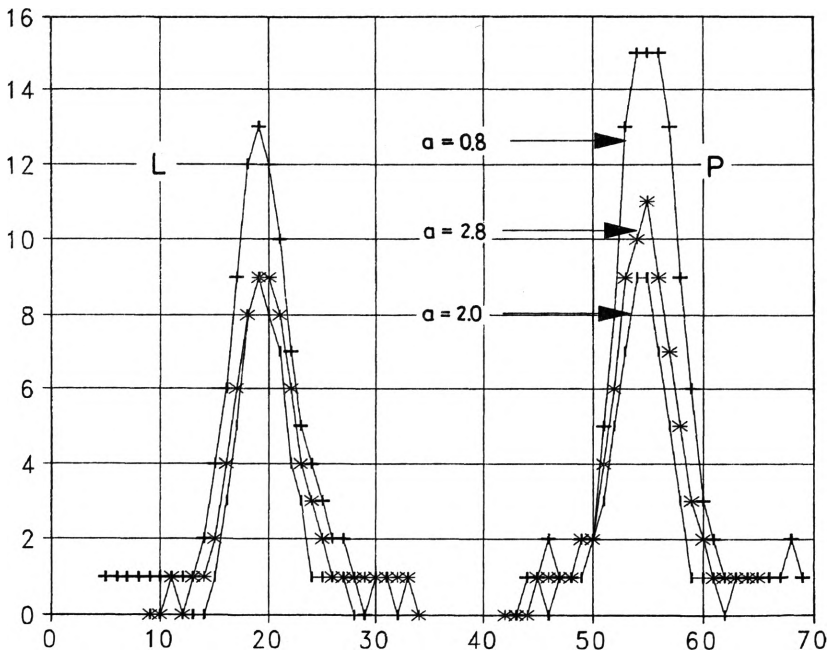


Fig. 7. Measured field distributions at the output of single mode Y junctions for the branching angles: $\alpha = 0.8^\circ, 2^\circ, 2.8^\circ$

After cutting and polishing the edges, substrate plates with waveguide structures were masked by the suitable layer of the silicon gum SILGEL 600. Next, the measurement window areas of the length of 1.75 cm each were uncovered in the measurement arms.

The basic elements of the waveguide structures described are Y junctions, the geometrical configurations and degree of asymmetry of which determine the working characteristics of the device. Interferometers were fabricated with different branching angles, varying from 0.8° to 5°. It assures the measurement and reference arm separation from 100 μm to 400 μm, respectively.

Figure 7 presents the measured near-field distributions at the output of single mode Y junctions for the branching angles $\alpha = 0.8^\circ, 2^\circ$ and 2.8° . Junctions in the examined range of angles work as power dividers. The degrees of the power division $I_1/(I_1 + I_2)$, where I_1 and I_2 denote powers in output ports, are equal to 54%, 55%, and 50%, respectively.

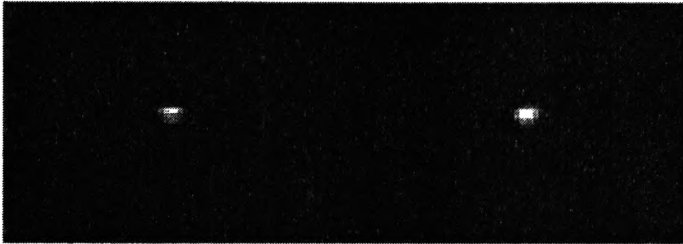


Fig. 8. Near-field pattern at the output of the Y junction of the branching angle $\alpha = 2.8^\circ$

Figure 8 shows a typical near-field pattern at the output of the Y junction ($\alpha = 2.8^\circ$) of the refractometer, which was chosen for further investigation.

4. Optical characteristics of the refractometer

The optical power at the output I_{out} of the symmetrical MZ interferometer can be expressed by the equation

$$I_{out} = \frac{I_{in}}{2} (1 + \cos(\Phi_m - \Phi_r)) \tag{2}$$

where I_{in} is optical power at the input, Φ_m and Φ_r denote the phase shift of the light transmitted in measurement m and reference r arms, respectively,

$$\Phi_{m,r} = 2\pi n_{eff,r,m} L/\lambda, \tag{3}$$

$n_{eff,r,m}$ is the effective refractive index of the guided modes in r or m arm, L is the arm length. In our case, the phase difference $\Phi_m - \Phi_r$ results from the dependence of the effective index of the mode in m arm on the refractive index of the cover in measurement area.

Optical characteristics of the refractometer were determined in the experimental set-up presented in Fig. 9. As the light source the LED (1.3 μm) was used, which was

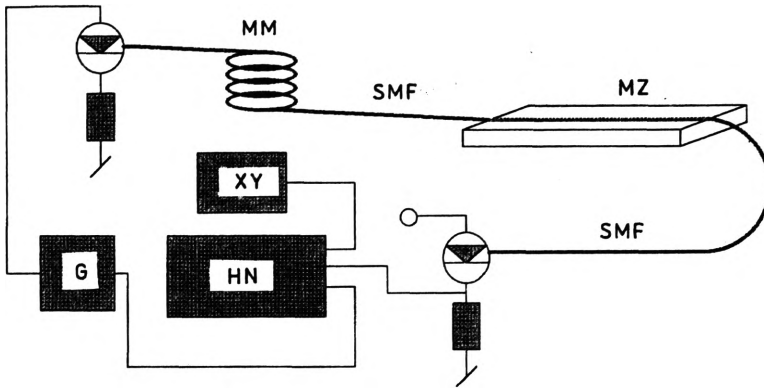


Fig. 9. Experimental set-up for measuring the optical characteristics of the refractometer: XY – recorder, HN – homodyne nanovoltmeter, MM – mode mixer, G – generator, SMF – single-mode fiber, MZ – Mach-Zehnder interferometer

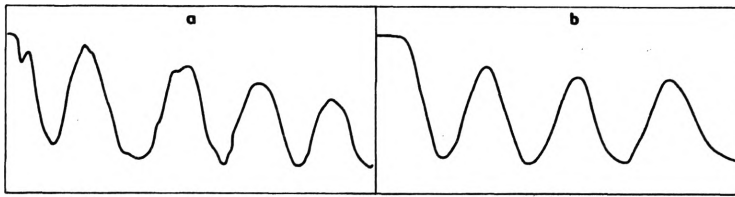


Fig. 10. Transmission characteristics of the refractometer as a function of the measurement area length (from 0 to 1.75 cm), for the refractive index of the cover: a – $n = 1.509$ and b – $n = 1.503$

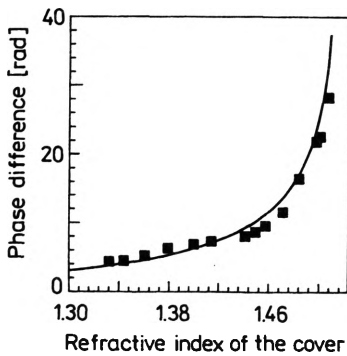


Fig. 11. Working curve of the planar refractometer

fed with a modulated signal from the generator G. Measurements with the planar refractometer were made using various test liquids of known refractive indices. The standard liquids were water solutions of glycerol and solutions of kerosene with bromonaphtalene whose light refraction indices changed within 1.33–1.51, measured at $\lambda = 0.589 \mu\text{m}$. Figure 10a, b, for example, presents transmission characteristics of the refractometer for the refractive index of the cover $n = 1.505$ and 1.503 as

a function of the measurement area length (from 0 to 1.75 cm). On the basis of an analysis of such transmission characteristics for all liquids tested, the working curve of the refractometer was determined. The results are shown in Fig. 11. The resolution of the refractometer obtained $d\Phi/dn$ changes from 45 rad at $n = 1.33$ to 457 rad at $n = 1.49$.

5. Conclusions

The planar refractometer presented in the paper, made in a symmetrical configuration of MZ interferometer, is characterized by high resolution, particularly for the refractive index of the cover near to the cut-off value. Further improvements are aimed to reduce the noise floor of the device. The refractometer described is designed for use in the planar optical sensors technology, especially chemical one, as a pH reaction sensor.

Acknowledgements — This work was partially supported by the Institute of Physics, Silesian Technical University, Poland, under project BW 94.

References

- [1] NAJAFI S. I., *Introduction to Glass Optics*, Artech House, Boston 1992.
- [2] GOTO N., YIP G. L., *Electron. Lett.* **26** (1990), 102.
- [3] MILIOU A. N., SRIVASTAVA R., RAMASWAMY R. V., *Appl. Opt.* **30** (1991), 674.
- [4] BŁAHUT M., OPILSKI A., ROGOZIŃSKI R., *Opt. Appl.* **22** (1992), 161.
- [5] HOCKER G. B., BURNS W. K., *Appl. Opt.* **16** (1977), 115.

Received June 27, 1994